

Late Quaternary variations in sea surface temperatures and their relationship to orbital forcing recorded in the Southern Ocean (Atlantic sector)

Uta Brathauer¹ and Andrea Abelmann

Alfred Wegener Institute for Polar and Marine Research, Bremerhaven, Germany

Abstract. Late Quaternary summer sea surface temperatures (SSTs) have been derived from radiolarian assemblages in the East Atlantic sector of the Southern Ocean. In the subantarctic and the polar frontal zone, glacial SSTs (oxygen isotope stages 2, 4, 6, and 8) were 3°-5°C cooler than today, indicating northward displacements of the isotherms about 2°-4° of latitudes. During interglacials, SSTs almost reached modern levels (oxygen isotope stages 7 and 9) or exceeded them by 2°-3°C (oxygen isotope stages 1 and 5.5). In the subantarctic Atlantic Ocean, changes in SST and calcium carbonate content of the sediment precede variations in global ice volume in the range of the main Milankovitch frequencies. Comparisons with the timing of North Atlantic Deep Water (NADW) proxy records suggests that this early response in the subantarctic Atlantic Ocean is not triggered by the flux of NADW to the Southern Ocean.

1. Introduction

The Southern Ocean is an important part in the global ocean circulation system. It connects the Pacific, the Atlantic, and the Indian Ocean and enables the exchange of water masses between these three ocean basins. As a major part in the global climate system, the determination of the Southern Ocean's role during the late Quaternary glaciation cycles contributes to the understanding of natural global climate change.

Since the work of *Hays et al.* [1976], it has been widely accepted that orbitally induced changes in geographical and seasonal distribution of insolation are a major cause of Pleistocene climatic changes, as earlier suggested by *Milankovitch* [1941]. It has also been recognized by *Hays et al.* [1976] and later confirmed by further studies [*Climate: Long-Range Investigation, Mapping, and Prediction (CLIMAP)*, 1984; *Imbrie et al.*, 1989, 1992; *Howard and Prell*, 1992; *Labeyrie et al.*, 1996] that Southern Ocean sea surface temperatures (SSTs) respond early to variations in Earth orbital parameters and lead changes in global ice volume. The causes of this "Southern Ocean lead" are still not clear. Changes in Southern Hemisphere insolation directly received by the Southern Ocean play only a minor role because of the large heat capacity of the ocean [*Short et al.*, 1991]. It has been suggested that the northern high-latitude insolation signal, which is critical for the onset of glaciation cycles [*Shackleton and Pisias*, 1985; *Imbrie et al.*, 1992, 1993; *Raymo*, 1997], is transmitted to the Southern Ocean via the North Atlantic Deep Water (NADW) and thus triggering the early response of southern SST [*Broecker*, 1984; *Imbrie et al.*, 1992].

Most of the knowledge about the late Quaternary Southern Ocean is based on sediment cores from the Indian sector. This study concentrates on the late Quaternary hydrographic changes in the Atlantic sector of the Southern Ocean, based on sea surface

temperature estimations derived from fossil radiolarian assemblages. Since the Climate: Long-Range Investigation, Mapping, and Prediction (CLIMAP) project, radiolarians have been established as a valuable tool for reconstructing SSTs in different parts of the world ocean. Several studies have shown that radiolarian SSTs provide comparable results to other SST proxies like alkenones, planktic foraminifera, coccoliths, or diatoms [*Molfini et al.*, 1982; *CLIMAP*, 1984; *Howard and Prell*, 1992; *Prahl et al.*, 1995; *Morley*, 1997; *Ortiz et al.*, 1997; *Pisias et al.*, 1997; *Abelmann et al.*, 1999]. In this work, a newly developed radiolarian based transfer function [*Abelmann et al.*, 1999] has been used to derive SST estimations from two sediment cores recovered in the subantarctic and the polar frontal zone, spanning the last 340 kyr and 200 kyr, respectively.

Furthermore, the derived subantarctic SST record has been analyzed in the frequency domain. For the main Milankovitch frequencies, the phase relationships to global ice volume have been determined. Comparisons between the phase angles of SST with those of other paleoclimatic indicators, e. g., calcium carbonate content of the sediment and NADW proxies, reveal information about the chain of events taking place during a changing climate and thus about the mechanisms within the climatic system.

2. Oceanographic Settings

Prominent features in the wind driven Antarctic Circumpolar Current (ACC) are the oceanic fronts, separating zonal bands within the ACC. From north to south these are the subtropical front, the subantarctic front, and the polar front (Figure 1). Several definitions based on surface or subsurface characteristics have been set up for the locations of the oceanic fronts [*Belkin and Gordon*, 1996]. *Lutjeharms and Valentine* [1984] showed that in the eastern Atlantic sector the positions of the oceanic fronts can be traced by thermal gradients in the sea surface hydrography alone. They found that the subtropical front, the northern boundary of the ACC, which separates the south Atlantic central water from the subantarctic surface water [*Peterson and Whitworth*, 1989; *Orsi et al.*, 1995], is characterized by a distinct temperature drop of approximately 7°C (from 18° to 11°C) over 225 km. On

¹Presently at GeoForschungsZentrum Potsdam, Potsdam, Germany.

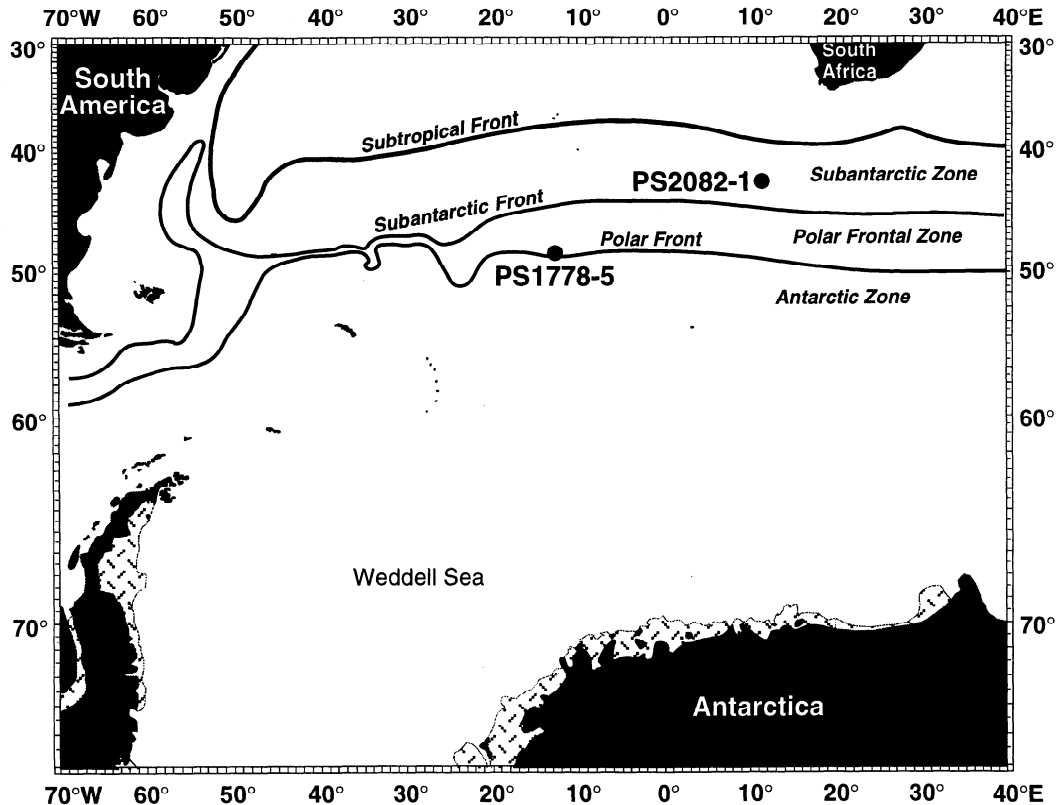


Figure 1. Locations of sediment cores PS2082-1 and PS1778-5. Frontal system after Peterson and Stramma [1991].

the basis of this surface expression, the geographic position of the subtropical front lies between 40°S and 42°S [Lutjeharms and Valentine, 1984]. The subantarctic front has been located between 45°S and 47°S, marked by a temperature drop of approximately 4°C (from 9° to 5°C) over 241 km [Lutjeharms and Valentine, 1984]. Finally, the polar front, which separates the Antarctic surface water from the subantarctic surface water [Whitworth and Nowlin, 1987; Peterson and Whitworth, 1989], exhibits the smallest gradient in sea surface temperature. The temperature decreases about 2°C (from 4° to 2°C) over 126 km. This front is located between 49°S and 50°S [Lutjeharms and Valentine, 1984].

3. Methods and Material

Two sediment cores have been examined in this study. Core PS2082-1 recovered in the subantarctic zone, between the subtropical front and the subantarctic front (43°13.2'S, 11°44.3'E), at a water depth of 4610 m, and core PS1778-5 recovered near the polar front (49°00.7'S, 12°41.8'W) at a water depth of 3380 m (Figure 1). Sediment core PS2082-1 has been sampled every 10 cm, and core PS1778-5 has been sampled every 10-20 cm for radiolarian faunal analysis. Slide preparation followed the Alfred Wegener Institute standard method [Abelmann, 1988, Abelmann *et al.* 1999]. On average, 400 individuals have been counted on each slide. A number of 187 radiolarian species and species groups have been identified [Brathauer, 1996].

Sea surface temperatures have been calculated using the transfer function method [Imbrie and Kipp, 1971] with a newly developed radiolarian transfer function for the East Atlantic sector of

the Southern Ocean [Abelmann *et al.*, 1999]. This transfer function is based on 23 radiolarian species or species groups in 52 sediment surface samples. Species selection was made on the basis of the modern distribution of radiolarians [e. g., Casey, 1971; Petrushevskaya, 1971a, b; Morley and Stepien, 1985; Kling and Boltovskoy, 1995; Abelmann and Gowing, 1996, 1997]. Only species which have been reported as surface dwelling have been selected for the transfer function, deep dwellers as well as no-analog species (e. g., *Cycladophora davisiana*) have been excluded. Thus the resulting transfer function represents surface water conditions. The surface sample data set spans a temperature range from -1° to 18°C in terms of modern mean summer sea surface temperatures. The modern SSTs have been extracted from the Southern Ocean atlas [Olbers *et al.*, 1992]. They represent mean summer sea surface temperatures (December-March) at 10 m depth. The standard error of estimate for this paleotemperature equation is 1.2°C. The details of the transfer function will be discussed by Abelmann *et al.* [1999].

Cross-spectral analyses were performed using the ARAND software package [Oregon State University (OSU) Computer Center Staff, 1973; Howell, 1989], which is based on the Blackman-Tukey method [Jenkins and Watts, 1968]. Calculations of coherency and phase angles have been achieved between parameters of core PS2082-1 and the SPECMAP stack. All time series have been transferred to equidistant sample intervals (2.5 kyr) via linear interpolation. The SPECMAP stack was reversed before the analyses; therefore maxima in $\delta^{18}\text{O}$ and thus minima in global ice volume are related with warm phases. The presentation of phase angles in phase wheels followed the SPECMAP conven-

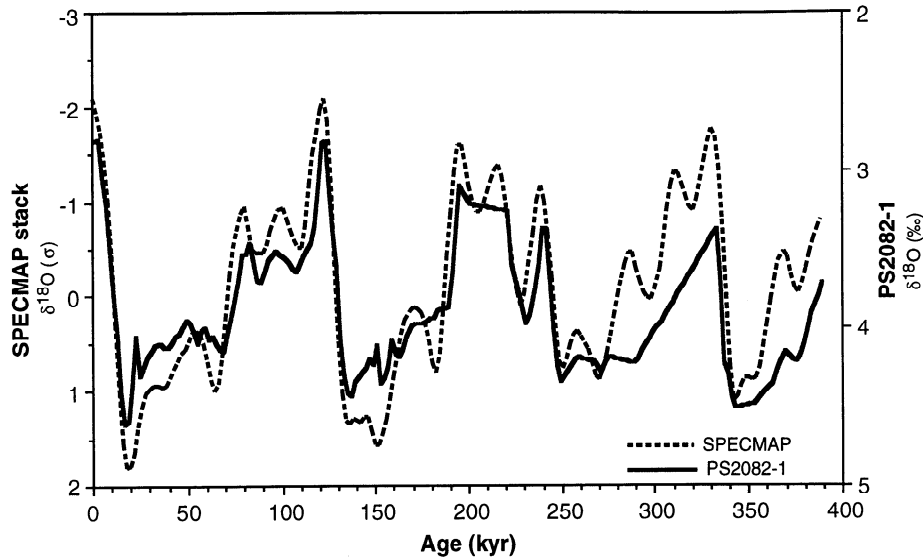


Figure 2. Comparison of the SPECMAP stack [Imbrie *et al.*, 1984] with the benthic foraminiferal $\delta^{18}\text{O}$ record of sediment core PS2082-1 [Mackensen *et al.*, 1994].

tion [Imbrie *et al.*, 1989]. The confidence levels for phases and coherencies were at 80% for all calculations.

4. Stratigraphy

An oxygen isotope stratigraphy has been established for sediment core PS2082-1 using isotopic measurements of benthic and planktic foraminifera [Mackensen *et al.*, 1994]. The record has been converted to SPECMAP ages [Imbrie *et al.*, 1984] (Figure 2), which resulted in a maximum age of about 390 ka [Mackensen *et al.*, 1994]. Cross-spectral analysis between the SPECMAP stack and the benthic foraminiferal $\delta^{18}\text{O}$ recorded in core PS2082-1 has been used to check the accuracy of this conversion [Imbrie *et al.*, 1989]. The results show that benthic foraminiferal $\delta^{18}\text{O}$ in core PS2082-1 is highly coherent (Figure 3) and in phase (Table 1) with the SPECMAP stack in the main Milankovitch bands ($1/100$, $1/41$, and $1/23 \text{ kyr}^{-1}$) as required for a successful conversion to SPECMAP timescale. A continuous *Cycladophora davisiana* record confirms the oxygen isotope stratigraphy for this core (Figure 4).

The age model for sediment core PS1778-5 is based on the *C. davisiana* stratigraphy solely. *C. davisiana* stages a to i_1 have been identified (Figure 4). They correspond to oxygen isotope stages 1 to late 7, spanning an age about 200 kyr [Hays *et al.*, 1976; Morley and Hays, 1979b]. SPECMAP ages have been assigned through graphic correlation of *C. davisiana* maxima and minima with the *C. davisiana* record of core PS2082-1 using AnalySeries software [Paillard *et al.*, 1996].

5. Results

5.1. Sea Surface Temperatures

Summer SSTs have been calculated for sediment cores PS2082-1 and PS1778-5 applying transfer function technique to radiolarian assemblages. Both cores exhibit distinct temperature

variations during late Quaternary glacial and interglacial stages. Core PS2082-1 recorded an average glacial cooling (oxygen isotope stages 2, 4, 6, and 8) about $4^\circ\text{-}5^\circ\text{C}$ for the subantarctic zone (Figure 5). In the polar frontal zone (PS1778-5), the average glacial cooling was somewhat less, about $3^\circ\text{-}4^\circ\text{C}$ (Figure 5). During the last glacial maximum (LGM), the sea surface temperatures in the subantarctic and polar frontal zones were $3^\circ\text{-}4^\circ\text{C}$ less than the modern values. During interglacials, the SST values in the subantarctic zone as well as in the polar frontal zone reached almost modern values (oxygen isotope stages 7 and 9) or even exceeded them by $2^\circ\text{-}3^\circ\text{C}$ (oxygen isotope stages 1 and 5.5) (Figure 5). Extreme changes in radiolarian SST occur at or just prior to terminations. During oxygen isotope stage transition 6/5 (termination II), the SST increased about $7^\circ\text{-}8^\circ\text{C}$, whereas at transitions 8/7 and 2/1 (terminations III and I), the SST increases are somewhat less (about $5^\circ\text{-}7^\circ\text{C}$) (Figure 5).

5.2. Time Series Analysis

Phases and coherency of benthic $\delta^{18}\text{O}$, %CaCO₃ of the sediment [Mackensen *et al.*, 1994] as well as radiolarian SST recorded in core PS2082-1 have been calculated against the reversed SPECMAP stack [Imbrie *et al.*, 1984] as an indicator for global ice volume. The benthic foraminiferal $\delta^{18}\text{O}$ spectra reveals discrete variance peaks in the $1/100$, $1/41$, and $1/23 \text{ kyr}^{-1}$ frequency ranges and the record is highly coherent and in phase with global ice volume in all three frequency bands (Figure 3, Table 1). The spectra of radiolarian summer SST also shows variance peaks in the $1/100$, $1/41$, $1/23$, and $1/19 \text{ kyr}^{-1}$ frequency ranges of the Milankovitch bands. The record is highly coherent with changes in global ice volume (Figure 6). Maxima in SST lead minima in global ice volume about $5.0 \pm 1.7 \text{ kyr}$ ($18^\circ \pm 6^\circ$) in the eccentricity cycle, $2.0 \pm 1.4 \text{ kyr}$ ($18^\circ \pm 12^\circ$) in the obliquity cycle, and $1.2 \pm 0.3 \text{ kyr}$ ($19^\circ \pm 5^\circ$) in the precession cycle (Table 1). The calcium carbonate variance spectra also exhibits main Milankovitch frequency peaks at $1/100$, $1/41$, and $1/23 \text{ kyr}^{-1}$ (Figure 6). As in the SST record, the maxima in calcium carbon-

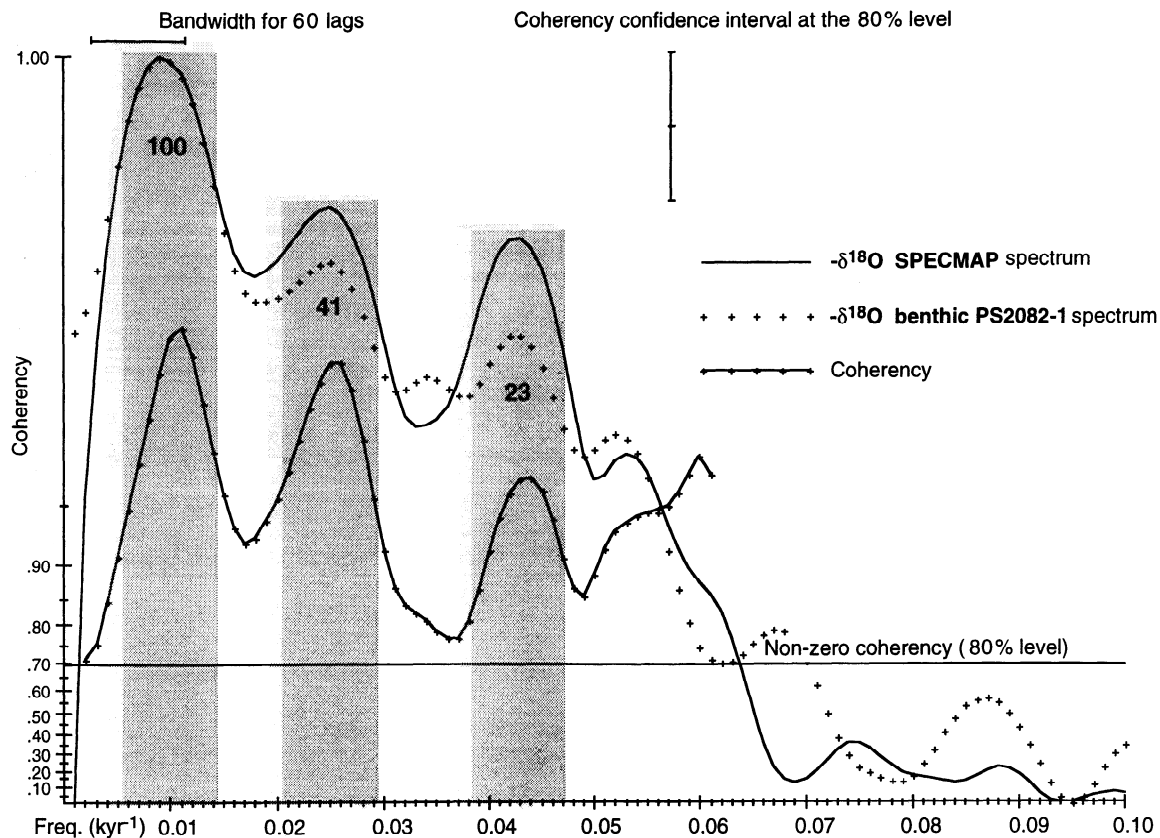


Figure 3. Results of cross-spectral analysis between the reversed SPECMAP stack [Imbrie *et al.*, 1984] and the reversed benthic foraminiferal $\delta^{18}\text{O}$ record of sediment core PS2082-1 [Mackensen *et al.*, 1994]. Shaded areas are equal to 1 bandwidth.

Table 1. Results of Cross-Spectral Analyses

Core	Data	k_0	$1/100 \text{ kyr}^{-1}$		$1/41 \text{ kyr}^{-1}$		$1/23 \text{ kyr}^{-1}$		b, cyc./kyr	T, kyr	ΔT , kyr
			k	Phi $^\circ$	k	Phi $^\circ$	k	Phi $^\circ$			
PS2082-1 (43 $^\circ$ S, 11 $^\circ$ E)	$-\delta^{18}\text{O}$ (benthic)	0.69	0.99	-3 \pm 3	0.99	6 \pm 4	0.96	1 \pm 8	0.009	388	2.5
PS2082-1 (43 $^\circ$ S, 11 $^\circ$ E)	SST (radiolaria)	0.73	0.97	-18 \pm 6	0.92	-18 \pm 12	0.99	-19 \pm 5	0.009	338	2.5
PS2082-1 (43 $^\circ$ S, 11 $^\circ$ E)	CaCO_3	0.64	0.83	-72 \pm 17	0.88	-33 \pm 14	0.92	-34 \pm 11	0.010	388	2.5
PS2082-1 (43 $^\circ$ S, 11 $^\circ$ E)	kaolinite/chlorite	0.64	0.96	-6 \pm 7	0.87	11 \pm 14	-	-	0.010	388	2.0
RC11-120/E49-18 (43 $^\circ$ S, 80 $^\circ$ E/46 $^\circ$ S, 90 $^\circ$ E)	SST (radiolaria)	0.66	0.92	-47 \pm 11	0.93	-14 \pm 10	0.86	-35 \pm 15	0.010	400	2.0
DSDP522/607/677 (56 $^\circ$ N, 23 $^\circ$ W), (41 $^\circ$ N, 33 $^\circ$ W), (1 $^\circ$ N, 84 $^\circ$ W)	NADW proxy (%ATL/PAC)	0.66	0.87	16 \pm 15	0.86	5 \pm 16	0.83	41 \pm 17	0.010	400	3.0
K708-1 (50 $^\circ$ N, 24 $^\circ$ W)	SST (foraminifera)	0.82	0.99	6 \pm 2	0.98	12 \pm 6	0.91	27 \pm 15	0.010	260	2.0

Variables are crossed with the reversed SPECMAP stack [Imbrie *et al.*, 1984]. Given are the nonzero coherency at the 80% level (k_0) as well as coherencies (k) and phase angles (Phi) with 80% confidence interval. Positive phases indicate that a variable lags; negative phases indicate that a variable leads the SPECMAP stack. Here b is bandwidth, T is maximum age of variable, ΔT is interpolation interval, and cyc. is cycles. References for data are PS2082-1, $\delta^{18}\text{O}$ (benthic) and CaCO_3 [Mackensen *et al.*, 1994]; PS2082-1, kaolinite/chlorite ratio [Diekmann *et al.*, 1996]; RC11-120, SST [Hays *et al.*, 1976]; NADW proxy (%ATLANTIC/PACIFIC) [Raymo *et al.*, 1990]; K708-1, SST [Ruddiman and McIntyre, 1984]. References for phases are RC11-120 (SST), NADW proxy (%ATLANTIC/PACIFIC), and K708-1 (SST) [Imbrie *et al.*, 1992]; PS2082-1 (kaolinite/chlorite ratio) [Diekmann *et al.*, 1996].

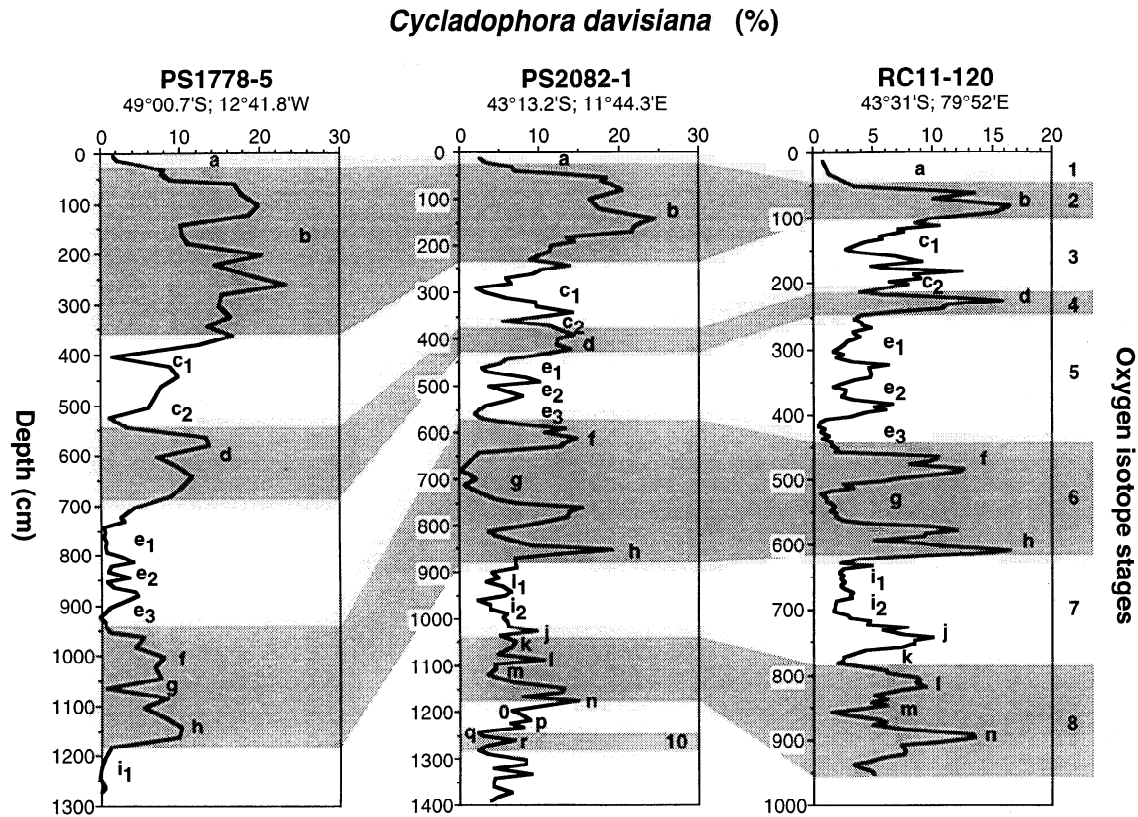


Figure 4. Relative abundances of *Cycladophora davisiana* in sediment cores PS1778-5, PS2082-1, and RC11-120 [Hays *et al.*, 1976] versus depth. Age models of cores PS2082-1 and RC11-120 are based on oxygen isotope stratigraphy [Howard and Prell, 1992; Mackensen *et al.*, 1994]. SPECMAP ages for core PS1778-5 have been assigned through correlation of that *C. davisiana* record with the one of core PS2082-1.

ate content lead minima in global ice volume, about 20 ± 4.7 kyr ($72^\circ \pm 17^\circ$) in the eccentricity cycle, 3.8 ± 1.6 kyr ($33^\circ \pm 14^\circ$) in the obliquity cycle, and 2.2 ± 0.7 kyr ($34^\circ \pm 11^\circ$) in the precession cycle (Table 1).

6. Discussion

6.1. Late Quaternary Sea Surface Temperature Distributions

In general, the pattern of radiolarian based SST records derived from sediment cores PS2082-1 and PS1778-5 in the Atlantic sector of the Southern Ocean are similar to other oceanic SST reconstructions from the tropical Atlantic [Imbrie *et al.*, 1989; Schneider *et al.*, 1995, 1996], the southern Indian Ocean [Howard and Prell, 1992; Pichon *et al.*, 1992; Labeyrie *et al.*, 1996], and the Atlantic sector of the Antarctic Ocean [Zielinski *et al.*, 1998] over the same time interval (Figure 5). Moreover, the radiolarian SST records are remarkably similar to variations in atmospheric SST as recorded in the δ -deuterium record of the Vostok ice core [Jouzel *et al.*, 1987, 1993, 1996] and to variations in the global $\delta^{18}\text{O}$ as documented in the SPECMAP stack [Imbrie *et al.*, 1984] (Figure 5).

Modern SST at the position of core PS2082-1 is about 11°C [Olbers *et al.*, 1992]. During oxygen isotope stage 2, sea surface temperatures dropped to 6° - 8°C (Figure 7). Today these temperatures are found south of the core's position in the area of the sub-

antarctic front. Thus it can be concluded that the isotherms of 6° - 8°C moved northward as far as the position of core PS2082-1 during oxygen isotope stage 2 (Figure 7). This variability in the SST distribution has been interpreted in terms of frontal movements, assuming the modern relationship between the summer sea surface temperature distribution and the position of the main oceanic fronts as described by Lutjeharms and Valentine [1984] and Lutjeharms *et al.* [1985]. Thus a northward migration of the subantarctic front over 2° - 4° of latitudes relative to the modern position can be inferred for oxygen isotope stage 2 (Figure 7). Similar results for the polar front can be deduced from core PS1778-5, which is located near the modern polar front (Figure 1). Recent SST is about 5°C [Olbers *et al.*, 1992]. During oxygen isotope stage 2, sea surface temperatures dropped to 1° - 4°C indicating a northward displacement of these isotherms and the polar front itself over 2° - 4° of latitudes (Figure 7).

The observed summer cooling of 3° - 4°C for the last glacial maximum in the subantarctic and polar frontal zones almost match the reconstructions of the CLIMAP group. They found a summer (February) cooling between 2° and 4°C for the East Atlantic sector of the Southern Ocean [CLIMAP, 1981]. On the basis of the SST records of sediment cores PS2082-1 and PS1778-5, northward movements of about 3° of latitudes for the subantarctic and the polar front can be estimated for the LGM. These values are also in the range of previous investigations. Morley and Hays [1979a] described a polar front migration about

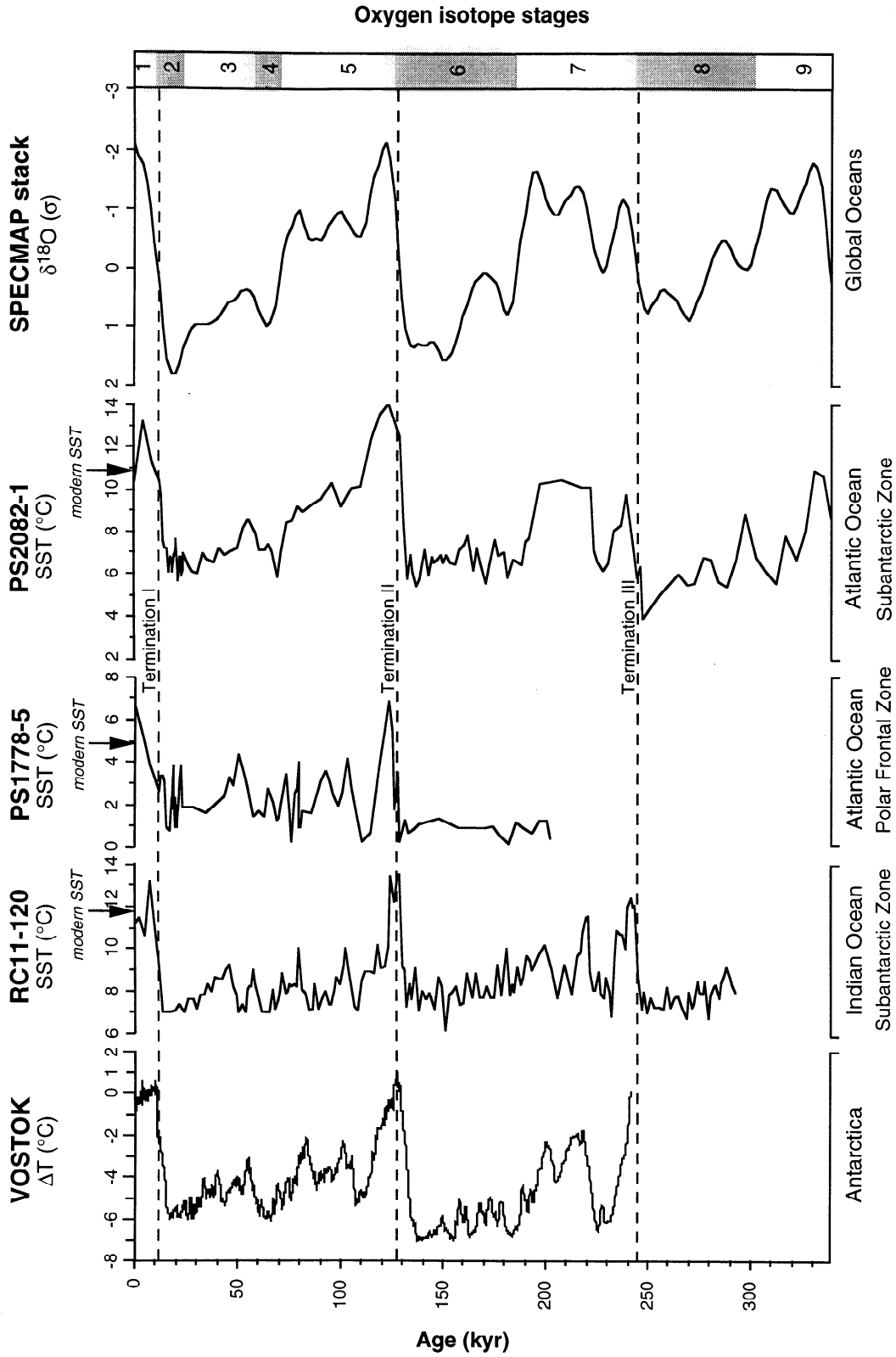


Figure 5. Late Quaternary summer SST changes in the Atlantic sector of the Southern Ocean (PS2082-1 and PS1778-5) in comparison with a summer SST record from the Indian sector of the Southern Ocean (RC11-120 [Hays *et al.*, 1976]), the atmospheric temperature record of the Vostok ice core expressed as difference to the modern annual temperature [Jouzel *et al.*, 1987, 1993, 1996], and the SPECMAP stack [Imbrie *et al.*, 1984].

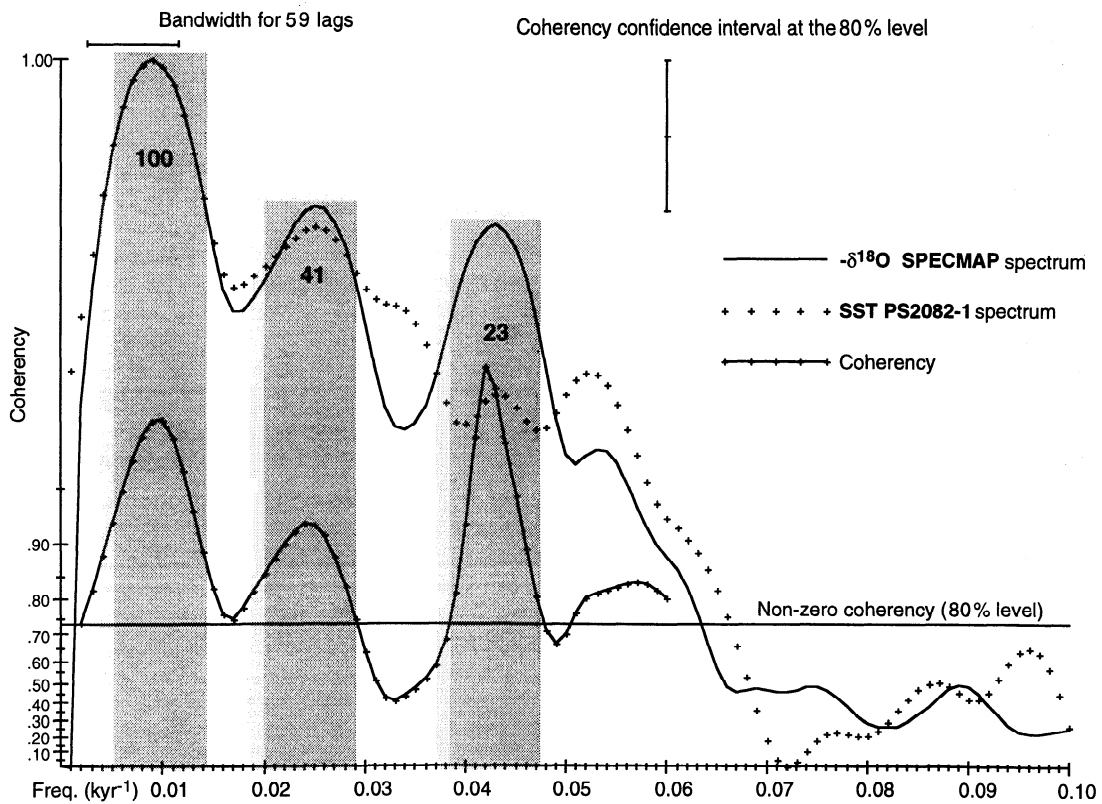
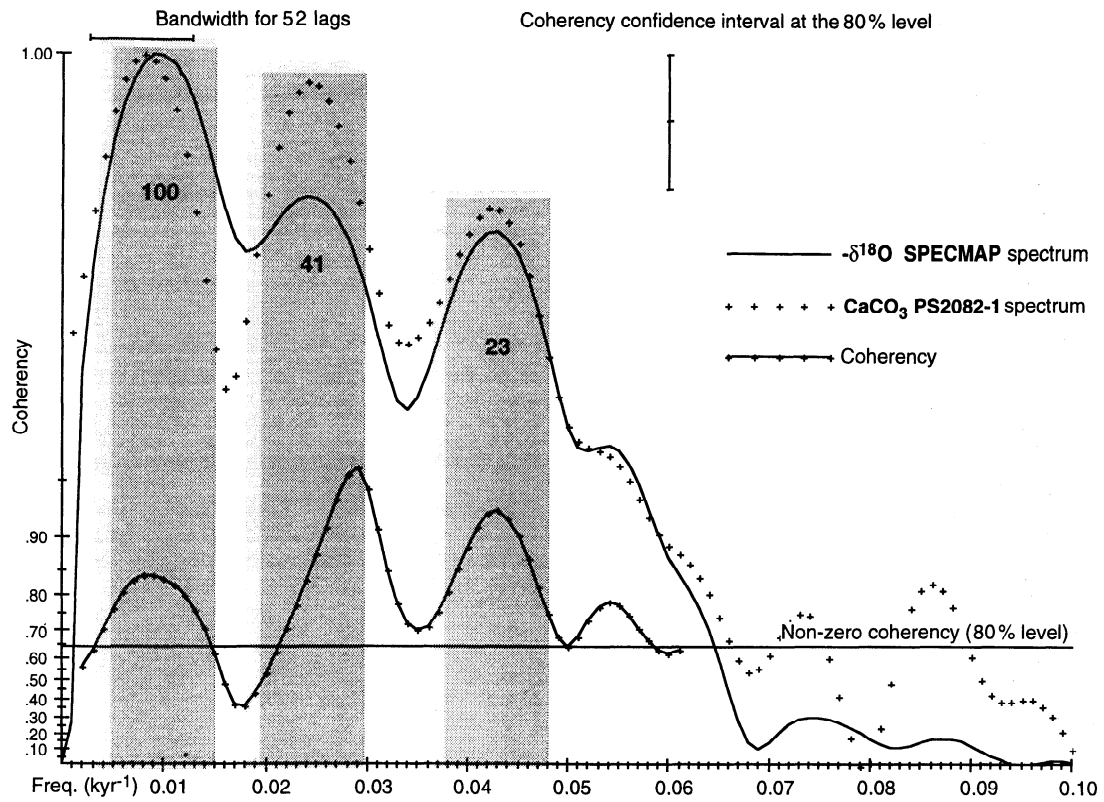


Figure 6. Results of cross-spectral analyses between the reversed SPECMAP stack [Imbrie *et al.*, 1984] and the CaCO_3 record [Mackensen *et al.*, 1994] as well as the radiolarian SST record of sediment core PS2082-1. Shaded areas are equal to 1 bandwidth.

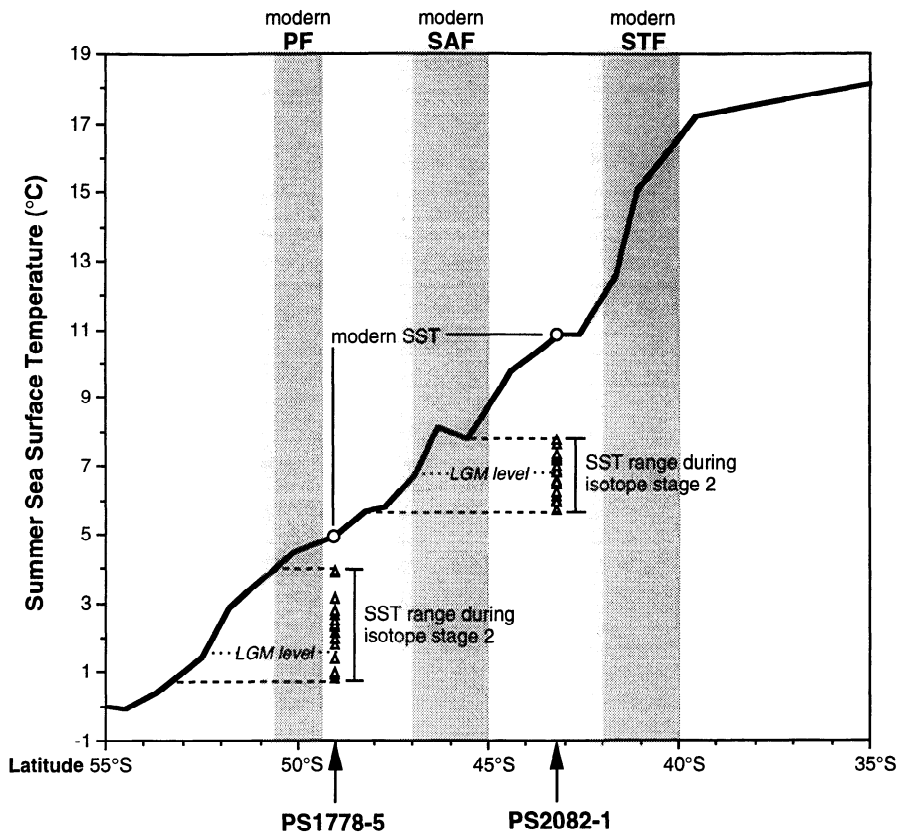


Figure 7. Summer SST ranges during oxygen isotope stage 2 in the subantarctic zone (PS2082-1) and the polar frontal zone (PS1778-5) in comparison with modern values. Modern SSTs are from *Obers et al.* [1992]. Shaded areas mark the modern ranges of the subtropical front (STF), the subantarctic front (SAF), and the polar front (PF) [*Lutjeharms and Valentine, 1984*].

1°-3° to the north for the eastern South Atlantic during the LGM. Recent investigations found values between 2° [*Niebler, 1995*] and 3° [*Nürnberg et al., 1997*] of latitudes. For the subantarctic front, *Niebler* [1995] estimated a northward displacement about 2° of latitudes.

Sea surface temperatures recorded during interglacial substage 5.5 are the warmest during the last 340 kyr (Figure 8). In the subantarctic zone, at the position of core PS2082-1, SST raised up to 14°C, which indicates southward displacements of the 14°C isotherm and the subtropical front over 2° of latitudes (Figure 8). In the polar frontal zone, the temperature signal of core PS1778-5 exhibits only one peak value distinctly higher than modern SSTs (5°C). The temperature raised up to 7°C, which indicates a southward displacement of the 7°C isotherm about 2° of latitudes (Figure 8).

The general pattern of latitudinal displacements show that most of time during the last 340 kyr the isotherms and the main oceanic fronts were north of their modern positions. Only during peak interglacial conditions the isotherms and oceanic fronts intended the same positions as today or moved southward in the East Atlantic sector of the Southern Ocean. The estimated frontal movements might be induced through changes in the position of wind fields as well as wind strengthening. Model experiments for the LGM show an increase of wind strength about 70% for Southern Hemisphere westerlies [*Lautenschlager and Herterich, 1990*]. This strengthening is also confirmed by paleo-data. On the basis

of aerosol content determinations in the Vostok ice core, *Petit et al.* [1981] suggested a wind strengthening about 50-80% for the subantarctic Glacial Ocean. LGM model results from *Kutzbach and Guetter* [1986] present a westwind drift movement about 5° north during austral summer. Model experiments from *Klinck and Smith* [1993] show that combining wind strengthening of 70% with a movement of wind fields about 5° to the north results in a more northward position (2°) of the Antarctic Circumpolar Current during the LGM. These model results are very close to the estimated frontal movements as described above.

6.2. The Role of Orbital Forcing in the Southern Ocean

Following the Milankovitch theory, the Pleistocene climatic changes are forced by orbitally induced insolation changes in northern high latitudes [*Milankovitch, 1941; Hays et al., 1976; Imbrie et al., 1989, 1992*]. Despite this, it has been detected that North Atlantic SST responds late, whereas the Southern Ocean SST responds early to variations in the Earth orbital parameters [*Hays et al., 1976; CLIMAP, 1984; Imbrie et al., 1989, 1992, 1993; Howard and Prell, 1992; Labeyrie et al., 1996*]. Besides SST, calcium carbonate preservation has also been detected in the early group of responses in cores from the Indian sector of the Southern Ocean [*Imbrie et al., 1992, 1993; Howard and Prell, 1994*]. The presented SST and CaCO₃ data from site PS2082-1 confirm the known "Southern Ocean lead" for the East Atlantic sector of the Southern Ocean (Table 1).

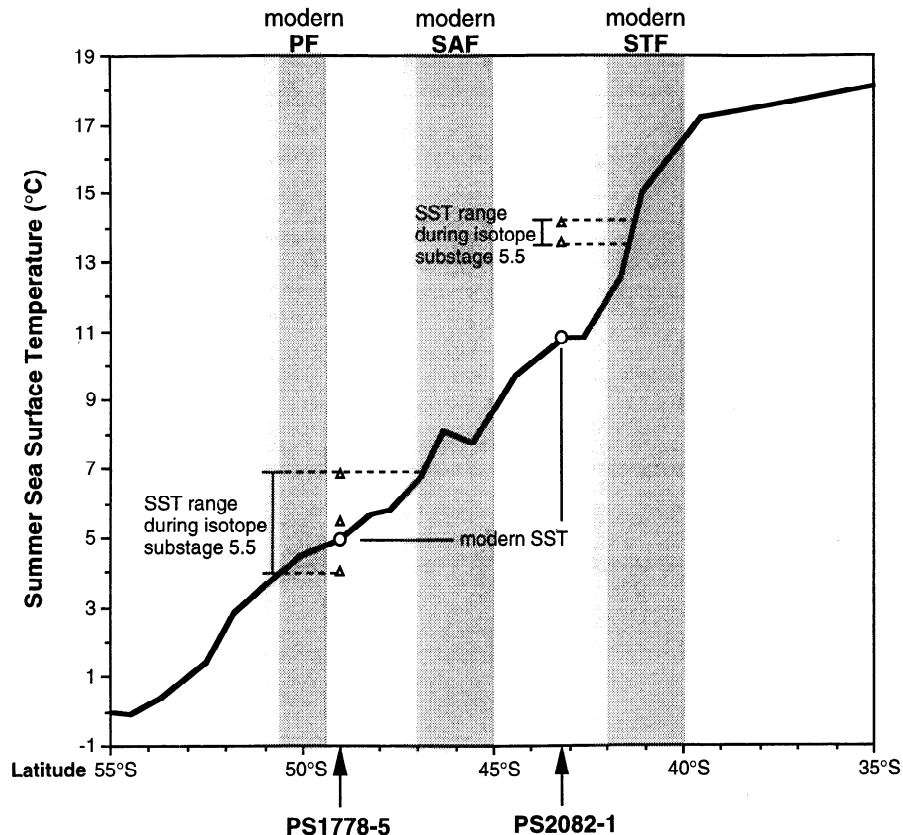


Figure 8. Summer SST ranges during oxygen isotope substage 5.5 in the subantarctic zone (PS2082-1) and the polar frontal zone (PS1778-5) in comparison with modern values. Modern SSTs are from *Olbers et al.* [1992]. Shaded areas mark the modern ranges of the subtropical front (STF), the subantarctic front (SAF), and the polar front (PF) [*Lutjeharms and Valentine, 1984*].

It has been postulated that the NADW is the transmitter of the Northern Hemisphere insolation signal to the Southern Ocean and triggers the early response of southern SST and calcium carbonate preservation [*Broecker, 1984; Imbrie et al., 1992; Howard and Prell, 1994*]. This explanation would require an early response of the NADW to insolation changes. However, observed phases of a NADW proxy record from *Raymo et al.* [1990] show that the NADW responds too late; it lags changes in Southern Ocean SST and calcium carbonate preservation in the range of the Milankovitch frequencies [*Howard and Prell, 1992; Imbrie et al., 1992, 1993; Howard and Prell, 1994*]. With respect to global ice volume, it lags in the 100 kyr and 23 kyr cycles and is almost in phase with global ice volume in the 41 kyr cycle (see Table 1).

Another NADW proxy, "the ratio of the clayminerals kaolinite and chlorite", has been determined in sediment core PS2082-1 (Figure 9a). This proxy is based on the finding that NADW carries pedogenic kaolinite from the tropical regions to the Southern Ocean, whereas chlorite originates from southern high latitudes and is transported by northward advection of southern-source deep water [*Diekmann et al., 1996*]. It has been shown that the latitudinal zonation of kaolinite/chlorite ratios in surface sediments reflect the distribution of deep water masses in the South Atlantic Ocean [*Diekmann et al., 1996; Petschick et al., 1996*]. High values of kaolinite/chlorite ratio display a penetration of NADW to the Southern Ocean. Cross-spectral results exhibit that this NADW proxy also lags Southern Ocean SST and CaCO_3

records from the same sediment core (PS2082-1) and that it is almost in phase with changes in global ice volume in the 100 and 41 kyr cycles [*Diekmann et al., 1996*] (Figure 9b). The 23 kyr cycle is not observed in the kaolinite/chlorite variance spectra, and thus a phase to global ice volume cannot be obtained.

On the basis of the described phase relationships, the production rate of NADW can be ruled out as the transmitter of the Northern Hemisphere insolation signal to the Southern Ocean. The phases of core PS2082-1 from the subantarctic Atlantic Ocean provide more evidence that the "Southern Ocean lead" (SST and CaCO_3) is not triggered by variations in the NADW.

The early response of calcium carbonate content of the sediment in Atlantic sector of the Southern Ocean in comparison to the late response of conveyor related NADW proxies (Figure 9b) is similar to the response of a carbonate preservation index from the Indian sector of the Southern Ocean [*Howard and Prell, 1994*]. *Howard and Prell* [1994] have shown that their Southern Ocean preservation index leads the NADW proxy record from *Raymo et al.* [1990] in the range of the main Milankovitch frequencies. These phase patterns point to the conclusion that the initial response in the calcium carbonate content of Southern Ocean sediments is not controlled by the decreased/increased transport of NADW to the Southern Ocean but instead by early local surface ocean processes. Such local processes, which are able to lower the glacial calcium carbonate content of Southern Ocean sediments might be a reduced glacial carbonate production

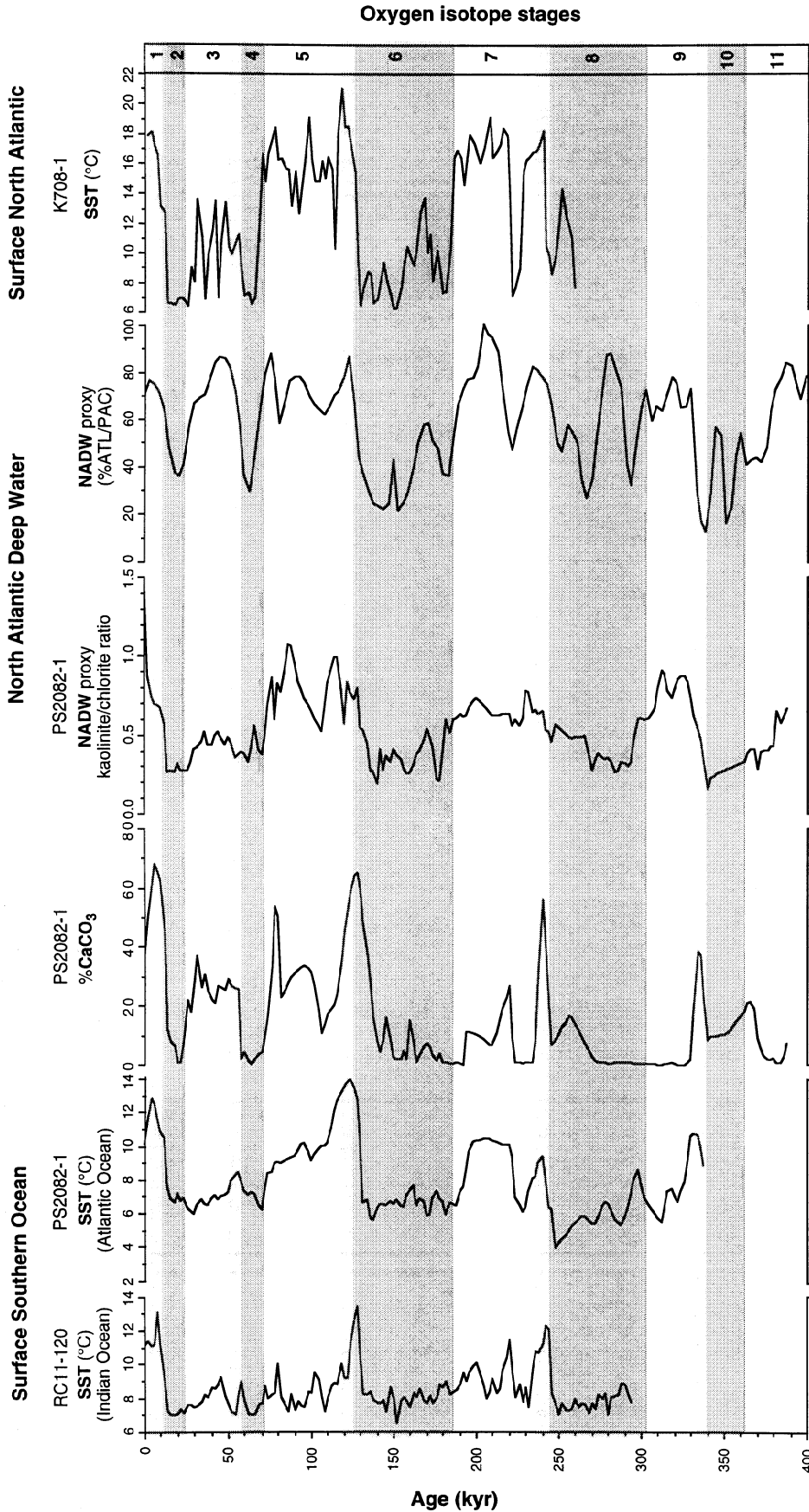


Figure 9a. Paleoclimate proxies, which have been included in phase diagrams, versus age. Records have been interpolated on equidistant intervals (see Table 1). References for data are RC11-120, SST [Hayes et al., 1976]; PS2082-1, CaCO₃ [Mackensen et al., 1994]; PS2082-1, kaolinite/chlorite ratio [Diekmann et al., 1996]; NADW proxy (%ATLANTIC/PACIFIC) [Raymo et al., 1990]; and K708-1, SST [Ruddiman and McIntyre, 1984].

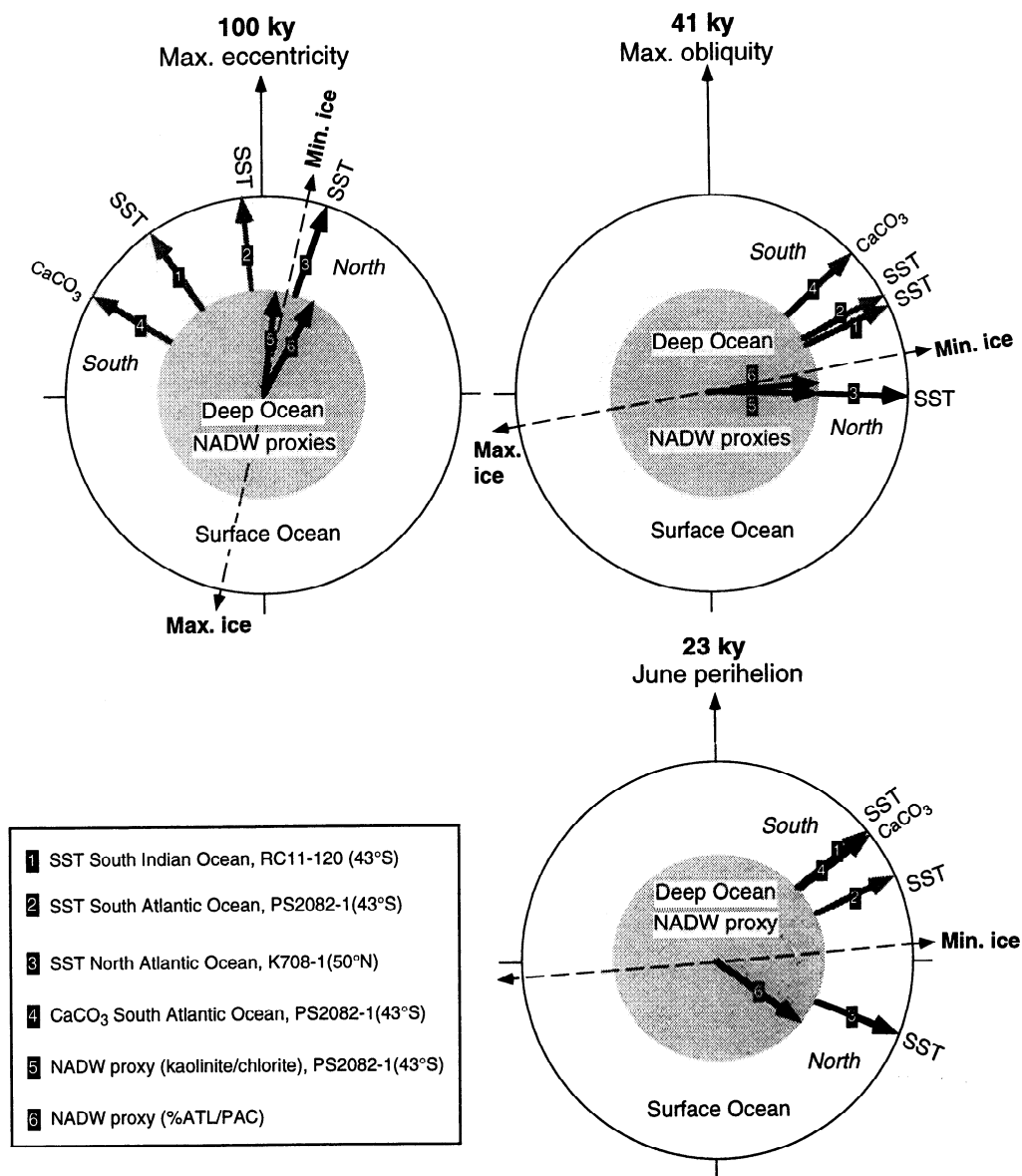


Figure 9b. Phase diagrams for paleoclimate proxies depicted in Figure 9a. Wheels are oriented after SPECMAP convention [Imbrie *et al.*, 1989]. The inner shaded circle shows phases for deep ocean NADW proxies; the outer circle gives the phases of surface ocean SST and CaCO_3 records. The SPECMAP stack has been taken as the indicator for global ice volume [Imbrie *et al.*, 1984, 1992]. References for data are RC11-120, SST [Hays *et al.*, 1976]; K708-1, SST [Ruddiman and McIntyre, 1984]; PS2082-1, CaCO_3 [Mackensen *et al.*, 1994]; PS2082-1, kaolinite/chlorite ratio [Diekmann *et al.*, 1996]; and NADW proxy (%ATLANTIC/PACIFIC) [Raymo *et al.*, 1990]. References for phases are RC11-120 (SST), NADW proxy (%ATLANTIC/PACIFIC), and K708-1 (SST) [Imbrie *et al.*, 1992]; PS2082-1 (kaolinite/chlorite ratio) [Diekmann *et al.*, 1996].

[Howard and Prell, 1994], maybe as a consequence of cooler surface temperatures which favor silica production instead of calcium carbonate production, and/or enhanced dissolution of CaCO_3 due to local enhanced organic carbon (C_{org}) productivity [Lea, 1995]. Higher glacial productivity in the area of core PS2082-1 has recently been presented by Kumar *et al.* [1995] and François *et al.* [1997]. Both reduced calcium carbonate production or higher C_{org} production lower the $\text{CaCO}_3/C_{\text{org}}$ rain ratios and thus causing enhanced calcium carbonate dissolution in the sediment [Archer, 1991; Archer and Maier-Reimer, 1994; Howard and Prell, 1994; Keir, 1995].

The finding that variations in the NADW influx to the Southern Ocean are not responsible for the Southern Ocean SST lead was earlier shown in the Indian sector of the Southern Ocean on orbital timescales [Labeyrie *et al.*, 1996] and in a nearby sediment core for millennial timescales [Charles *et al.*, 1996]. The remaining question is still what triggers the early response of the southern SST signal, if it is not caused by variations in NADW flux? An explanation lies perhaps in the different driving mechanisms of surface circulation and deep water circulation. The Southern Ocean surface circulation is wind driven, whereas the deep water circulation depends on temperature and salinity contrasts. Thus

the lead of Southern Ocean surface waters (SST) might be caused by early changes in the atmosphere and wind fields, as earlier suggested by *Labeyrie et al.* [1996], whereas the lagged response of conveyor related proxies in the Southern Ocean deep water (kaolinite/chlorite ratio) might be due to the later response of NADW which is in phase with or lags Northern Hemisphere ice sheets [*Raymo et al.*, 1990; *Howard and Prell*, 1992].

The leading pattern of SST is not restricted to southern Indian and Atlantic Ocean; it has also been reported from the equatorial Atlantic [*Imbrie et al.*, 1989; *Schneider et al.*, 1995] and recently from the equatorial Pacific [*Pisias and Mix*, 1997]. Moreover, the atmospheric temperatures as recorded in the δ -deuterium record of the Vostok ice core as well lead global ice volume [*Waelbroeck et al.*, 1995]. This reflects a close connection between Southern Hemisphere atmospheric circulation and Southern Hemisphere ocean surface circulation and points to atmospheric circulation as a driver of early Southern Ocean surface temperature changes. Atmospheric circulation provides a clear link between the different ocean basins of the Southern Hemisphere, Vostok, and the Northern high latitudes, which are critical for the onset of glacial/interglacial cycles [*Shackleton and Pisias*, 1985; *Imbrie et al.*, 1992, 1993; *Raymo*, 1997]. Furthermore, atmospheric circulation can be altered externally through orbitally induced seasonal and latitudinal variations in insolation [*Kutzbach and Guetter*, 1986]. The different response times between the lagging North Atlantic SST and the leading Southern Ocean SST (Figure 9a, b and Table 1) might be due to different environmental conditions. The Southern Hemisphere is dominated by oceans. Surface ocean temperature can immediately respond to changes in atmospheric circulation [*Webb et al.*, 1993], for example, wind driven changes in positions of oceanic fronts [*Labeyrie et al.*, 1996]. Whereas in the Northern Hemisphere, the response of the entire system, atmosphere, North Atlantic surface and deep-ocean, is lagged by the dominating control of Northern Hemisphere ice sheets [*Ruddiman and McIntyre*, 1984; *Imbrie et al.*, 1989; *Ruddiman et al.*, 1989; *Webb et al.*, 1993]. Owing to the lagged response of NADW, which drives ocean thermohaline circulation, the Southern Ocean deep water proxies (kaolinite/chlorite ratio) as well react late to changes in Earth orbital parameters.

7. Summary and Conclusions

Late Quaternary variations in summer sea surface temperatures in the East Atlantic sector of the Southern Ocean have been

reconstructed from fossil radiolarian assemblages using transfer function technique. During glacial times (oxygen isotope stages 2, 4, 6, and 8), the surface of the ocean in the subantarctic and the polar frontal zone was 3°-5°C cooler than today, indicating a northward displacement of isotherms about 2°-4° of latitudes with respect to modern positions. During interglacials, sea surface temperatures almost reached modern levels (oxygen isotope stages 7 and 9) or exceeded them by 2°-3°C (oxygen isotope stages 1 and 5.5).

Interpreted in terms of frontal movements, the observed summer cooling of 3°-4°C during the last glacial maximum indicates northward migrations of the subantarctic and the polar front about 3° of latitudes relative to their modern positions. The warming of the subantarctic surface ocean during oxygen isotope substage 5.5 might be related to a southward movement of the subtropical front over 2° of latitudes.

Cross-spectral analyses show that changes in subantarctic SST and calcium carbonate content of the sediment, as recorded in core PS2082-1, precede variations in global ice volume in the range of the main Milankovitch bands. In contrast, proxy records of NADW are in phase or lag changes in global ice volume. These phase relationships suggest that this early response in the subantarctic Atlantic Ocean is not triggered by the flux of NADW to the Southern Ocean.

Acknowledgments. We thank our colleagues Dieter Fütterer, Rainer Gersonde, Andreas Mackensen, and Ulrich Zielinski for valuable comments and helpful discussions throughout this study. U. Brathauer is thankful to Nicklas Pisias for the introduction to time series analysis and his support and hospitality during her stay at Oregon State University. We are also grateful to Rainer Sieger, who assisted with computer problems and wrote a counting program for microfossils. For the preparation of radiolarian slides, we are indebted to Inge Klappstein. We thank Xavier Crosta and two anonymous reviewers for their helpful comments on the original manuscript. A part of this work was funded by a grant of the "Deutscher Akademischer Austauschdienst" to U. Brathauer. This is Alfred Wegener Institute publication No. 1538 and Sonderforschungsbereich 261 publication No. 263. Presented summer SST data for cores PS1778-5 and PS2082-1 as well as the age model for core PS1778-5 will be stored in the Pangaea database (www.pangaea.de) and the World Data Center-A for Paleoclimatology (www.ngdc.noaa.gov/paleo).

References

- Abelmann, A., Freeze-drying simplifies the preparation of microfossils, *Micropaleontology*, 34, 361, 1988.
- Abelmann, A., U. Brathauer, R. Gersonde, R. Sieger, and U. Zielinski, Radiolarian-based transfer function for the estimation of sea-surface temperatures in the Southern Ocean (Atlantic sector), *Paleoceanography*, in press, 1999.
- Abelmann, A., and M. M. Gowing, Horizontal and vertical distribution pattern of living radiolarians along a transect from the Southern Ocean to the South Atlantic Subtropical region, *Deep Sea Res., Part 1*, 43, 361-382, 1996.
- Abelmann, A., and M. M. Gowing, Spatial distribution pattern of living polycystine radiolarian taxa - Baseline study for paleoenvironmental reconstructions in the Southern Ocean (Atlantic sector), *Mar. Micropaleontology*, 30, 3-28, 1997.
- Archer, D., Modeling the calcite lysocline, *J. Geophys. Res.*, 96, 17037-17050, 1991.
- Archer, D., and E. Maier-Reimer, Effect of deep-sea sedimentary calcite preservation on atmospheric CO₂ concentration, *Nature*, 367, 260-263, 1994.
- Belkin, I. G., and A. L. Gordon, Southern Ocean fronts from Greenwich meridian to Tasmania, *J. Geophys. Res.*, 101, 3675-3696, 1996.
- Brathauer, U., Radiolarians as indicators for Quaternary climatic changes in the Southern Ocean (Atlantic Sector) (in German with English abstract), *Reports on Polar Research, rep. 216*, pp. 1-163, Alfred Wegener Inst. for Polar and Mar. Res., Bremerhaven, Germany, 1996.
- Broecker, W. S., Terminations, in *Milankovitch and Climate Part 2*, edited by A. Berger et al., pp. 687-698, D. Reidel, Norwell, Mass., 1984.
- Casey, R. E., Radiolarians as indicators of past and present water-masses, in *Micropaleontology of Oceans*, edited by B. M. Funnell and W. R. Riedel, pp. 331-341, Cambridge University Press, New York, 1971.
- Charles, C. D., J. Lynch-Stieglitz, U. S. Ninnemann, and R. G. Fairbanks, Climate

- connections between the hemisphere revealed by deep sea sediment core/ice core correlations, *Earth Planet. Sci. Lett.*, *142*, 19-27, 1996.
- Climate: Long-Range Investigation, Mapping, and Prediction (CLIMAP), Seasonal reconstructions of the Earth's surface at the last glacial maximum, *Map and Chart Ser. MC-36*, pp. 1-18, Geol. Soc. Am., Boulder, Colo., 1981.
- Climate: Long-Range Investigation, Mapping, and Prediction (CLIMAP), The last interglacial ocean, *Quat. Res.*, *21*, 123-224, 1984.
- Diekmann, B., R. Petschick, F. X. Gingle, D. K. Fütterer, A. Abelmann, U. Brathauer, R. Gersonde, and A. Mackensen, Clay mineral fluctuations in late Quaternary sediments of the southeastern South Atlantic: Implications for past changes of deep water advection, in *The South Atlantic: Present and Past Circulation*, edited by G. Wefer et al., pp. 621-644, Springer-Verlag, New York, 1996.
- François, R., M. A. Altabet, E.-F. Yu, D. M. Sigman, M. P. Bacon, M. Frank, G. Bohrmann, G. Bareille, and L. D. Labeyrie, Contribution of Southern Ocean surface-water stratification to low atmospheric CO₂ concentrations during the last glacial period, *Nature*, *389*, 929-935, 1997.
- Hays, J. D., J. Imbrie, and N. J. Shackleton, Variations in the Earth's orbit: Pacemaker of the ice ages, *Science*, *194*, 1121-1132, 1976.
- Howard, W. R., and W. L. Prell, Late Quaternary surface circulation of the southern Indian Ocean and its relationship to orbital variations, *Paleoceanography*, *7*, 79-117, 1992.
- Howard, W. R., and W. L. Prell, Late Quaternary CaCO₃ production and preservation in the Southern Ocean: Implications for oceanic and atmospheric carbon cycling, *Paleoceanography*, *9*, 453-482, 1994.
- Howell, P., *ARAND Programs for Macintosh*, Brown Univ., Providence, R. I., 1989.
- Imbrie, J., and N. G. Kipp, A new micropaleontological method for quantitative paleoclimatology: application to a late Pleistocene Caribbean core, in *The Late Cenozoic Glacial Ages*, edited by K. K. Turekian, pp. 71-181, Yale Univ. Press, New Haven, Conn., 1971.
- Imbrie, J., J. D. Hays, D. G. Martinson, A. McIntyre, A. C. Mix, J. J. Morley, N. G. Pisias, W. L. Prell, and N. J. Shackleton, The orbital theory of Pleistocene climate: Support from a revised chronology of the marine $\delta^{18}\text{O}$ record, in *Milankovitch and Climate Part 1*, edited by A. Berger et al., pp. 269-305, D. Reidel, Norwell, Mass., 1984.
- Imbrie, J., A. McIntyre, and A. Mix, Oceanic response to orbital forcing in the late Quaternary: Observational and experimental strategies, in *Climate and Geo-Sciences, A Challenge for Science and Society in the 21st Century*, edited by A. Berger, S. Schneider, and J.-C. Duplessy, pp. 121-164, Kluwer Acad., Norwell, Mass., 1989.
- Imbrie, J. et al., On the structure and origin of major glaciation cycles, 1, Linear responses to Milankovitch forcing, *Paleoceanography*, *7*, 701-738, 1992.
- Imbrie, J. et al., On the structure and origin of major glaciation cycles, 2, The 100,000-year cycle, *Paleoceanography*, *8*, 699-735, 1993.
- Jenkins, G. M. and D. G. Watts, *Spectral Analysis and its Applications*, 525 pp., Holden-Day, Merrifield, Va., 1968.
- Jouzel, J., C. Lorius, J. R. Petit, C. Genthon, N. I. Barkov, V. M. Kotlyakov, and V. M. Petrov, Vostok ice core: A continuous isotope temperature record over the last climatic cycle (160,000), *Nature*, *329*, 403-408, 1987.
- Jouzel, J. et al., Extending the Vostok ice-core record of paleoclimate to the penultimate glacial period, *Nature*, *364*, 407-412, 1993.
- Jouzel, J. et al., Climatic interpretation of the recently extended Vostok ice records, *Clim. Dyn.*, *12*, 513-521, 1996.
- Keir, R. S., Is there a component of Pleistocene CO₂ change associated with carbonate dissolution cycles?, *Paleoceanography*, *10*, 871-880, 1995.
- Klinck, J. M., and D. A. Smith, Effect of wind changes during the last glacial maximum on the circulation in the Southern Ocean, *Paleoceanography*, *8*, 427-433, 1993.
- Kling, S. A., and D. B. Boltovskoy, Radiolarian vertical distribution patterns across the southern California current, *Deep Sea Res., Part 1*, *42*, 191-231, 1995.
- Kumar, N., R. F. Anderson, R. A. Mortlock, P. N. Froelich, P. Kubik, B. Ditttrich-Hannen, and M. Suter, Increased biological productivity and export production in the glacial Southern Ocean, *Nature*, *378*, 675-680, 1995.
- Kutzbach, J. E., and P. J. Guetter, The influence of changing orbital parameters and surface boundary conditions for the past 18,000 years, *J. Atmos. Sci.*, *43*, 1726-1759, 1986.
- Labeyrie, L. et al., Hydrographic changes of the Southern Ocean (southeast Indian sector) over the last 230 kyr, *Paleoceanography*, *11*, 57-76, 1996.
- Lautenschlager, M., and K. Herterich, Atmospheric response to ice age conditions: Climatology near the Earth's surface, *J. Geophys. Res.*, *95*, 22547-22557, 1990.
- Lea, D. W., A trace metal perspective on the evolution of Antarctic Circumpolar Deep Water chemistry, *Paleoceanography*, *10*, 733-747, 1995.
- Lutjeharms, J. R. E., and H. R. Valentine, Southern Ocean thermal fronts south of Africa, *Deep Sea Res., Part A*, *31*, 1461-1475, 1984.
- Lutjeharms, J. R. E., M. N. Walters, and B. R. Allanson, Oceanic frontal systems and biological enhancement, in *Antarctic Nutrient Cycles and Food Webs*, edited by W. R. Siegfried, P. R. Condy, and R. M. Laws, pp. 11-21, Springer-Verlag, New York, 1985.
- Mackensen, A., H. Grobe, H.-W. Hubberten, and G. Kuhn, Benthic foraminiferal assemblages and the $\delta^{13}\text{C}$ -signal in the Atlantic sector of the Southern Ocean: Glacial-to-interglacial contrasts, in *Carbon Cycling in the Glacial Ocean: Constraints on the Ocean's Role in Global Change*, edited by R. Zahn et al., pp. 104-144, Springer-Verlag, New York, 1994.
- Milankovitch, M., *Kanon der Erdbeinstrahlung und seine Anwendung auf das Eiszeitenproblem*, *J. Serb. Acad., Belgrad, Spec. Publ.*, *133*, 1-633, 1941.
- Molfino, B., N. G. Kipp, and J. J. Morley, Comparison of foraminiferal, coccolithophorid, and radiolarian paleotemperature equations: Assemblage coherency and estimate concordancy, *Quat. Res.*, *17*, 279-313, 1982.
- Morley, J. J., Variations in the California Current system at 34°N between 65 and 140 ka: Evidence from multiple paleoceanographic indices from the Santa Barbara Basin, *EOS, Trans. AGU*, *78* (46), Fall Meet. Suppl., f377, 1997.
- Morley, J. J., and J. D. Hays, Comparison of glacial and interglacial oceanographic conditions in the South Atlantic from variations in calcium carbonate and radiolarian distributions, *Quat. Res.*, *12*, 396-408, 1979a.
- Morley, J. J., and J. D. Hays, *Cycladophora davisiana*: A stratigraphic tool for Pleistocene North Atlantic and interhemispheric correlation, *Earth Planet. Sci. Lett.*, *44*, 383-389, 1979b.
- Morley, J. J., and J. C. Stepien, Antarctic radiolaria in late winter/early spring Weddell Sea waters, *Micropaleontology*, *31*, 365-371, 1985.
- Niebler, H.-S., Reconstruction of paleo-environmental parameters using stable isotopes and faunal assemblages of planktonic foraminifera in the South Atlantic Ocean (in German with English abstract), *Reports on Polar Research, rep. 167*, pp. 1-198, Alfred Wegener Inst. for Polar and Mar. Res., Bremerhaven, Germany, 1995.
- Nürnberg, C. C., G. Bohrmann, and M. Schlüter, Barium accumulation in the Atlantic sector of the Southern Ocean: Results from 190,000-year records, *Paleoceanography*, *12*, 594-603, 1997.
- Olbers, D., V. Gouretski, G. Seiß, and J. Schröter, *Hydrographic Atlas of the Southern Ocean*, 82 pp., Alfred Wegener Inst. for Polar and Mar. Res., Bremerhaven, Germany, 1992.
- Oregon State University (OSU) Computer Center Staff, *ARAND Routines and Programs*, Oregon State Univ., Corvallis, 1973.
- Orsi, A. H., T. Whitworth III, and W. D. Nowlin Jr., On the meridional extent and fronts of the Antarctic Circumpolar Current, *Deep-Sea Res., Part 1*, *42*, 641-673, 1995.
- Ortiz, J., A. Mix, S. Hostetler, and M. Kashgarian, The California Current of the last glacial maximum: Reconstruction at 42°N based on multiple proxies, *Paleoceanography*, *12*, 191-205, 1997.
- Paillard, D., L. Labeyrie, and P. Yiou, Macintosh program performs time-series analysis, *EOS Trans. AGU*, *77*, 379, 1996.
- Peterson, R. G., and L. Stramma, Upper-level circulation in the South Atlantic Ocean, *Prog. Oceanogr.*, *26*, 1-73, 1991.
- Peterson, R. G., and T. Whitworth III, The subantarctic and polar fronts in relation to deep water masses through the southwestern Atlantic, *J. Geophys. Res.*, *94*, 10817-10838, 1989.
- Petit, J.-R., M. Briat, and A. Royer, Ice age aerosol content from East Antarctic ice core samples and past wind strength, *Nature*, *293*, 391-394, 1981.
- Petrushevskaya, M. G., Radiolaria in the plankton and recent sediments from the Indian Ocean and Antarctic, in *Micropaleontology of Oceans*, edited by W. R. Riedel, pp. 319-329, Cambridge Univ. Press, New York, 1971a.
- Petrushevskaya, M. G., Radiolarians of the World Ocean: According to the data of Soviet

- expeditions, in *Investigations of the Fauna of the Seas IX (XVII)*, edited by B. E. Bykhovskij, pp. 5-294, Acad. Sci. USSR, Inst. Zool., Leningrad, Russia, 1971b.
- Petschick, R., G. Kuhn, and F. Gingele, Clay mineral distribution in surface sediments of the South Atlantic: Sources, transport, and relation to oceanography, *Mar. Geol.*, *130*, 203-229, 1996.
- Pichon, J. J., L. D. Labeyrie, G. Bareille, M. Labracherie, J. Duprat, and J. Jouzel, Surface water temperature changes in the high latitudes of the Southern Hemisphere over the last glacial-interglacial cycle, *Paleoceanography*, *7*, 289-318, 1992.
- Pisias, N. G., and A. C. Mix, Spatial and temporal oceanographic variability of the eastern equatorial Pacific during the late Pleistocene: Evidence from Radiolaria microfossils, *Paleoceanography*, *12*, 381-393, 1997.
- Pisias, N. G., A. Roelofs, and M. Weber, Radiolarian-based transfer functions for estimating mean surface ocean temperatures and seasonal range, *Paleoceanography*, *12*, 365-379, 1997.
- Prahl, F. G., N. Pisias, M. A. Sparrow, and A. Sabin, Assessment of sea-surface temperature at 42°N in the California Current over the last 30,000 years, *Paleoceanography*, *10*, 763-773, 1995.
- Raymo, M. E., The timing of major climate terminations, *Paleoceanography*, *12*, 577-585, 1997.
- Raymo, M. E., W. F. Ruddiman, N. J. Shackleton, and D. W. Oppo, Evolution of Atlantic-Pacific $\delta^{13}\text{C}$ gradients over the last 2.5 m.y., *Earth Planet. Sci. Lett.*, *97*, 353-368, 1990.
- Ruddiman, W. F., and A. McIntyre, Ice-age thermal response and climatic role of the surface Atlantic Ocean, 40°N to 63°N, *Geol. Soc. Am. Bull.*, *95*, 381-396, 1984.
- Ruddiman, W. F., M. E. Raymo, D. G. Martinson, B. M. Clement, and J. Backman, Pleistocene evolution: Northern Hemisphere ice sheets and North Atlantic Ocean, *Paleoceanography*, *4*, 353-412, 1989.
- Schneider, R. R., P. J. Müller, and G. Ruhland, Late Quaternary surface circulation in the east equatorial South Atlantic: Evidence from alkenone sea surface temperatures, *Paleoceanography*, *10*, 197-219, 1995.
- Schneider, R. R., P. J. Müller, G. Ruhland, G. Meinecke, H. Schmidt, and G. Wefer, Late Quaternary surface temperatures and productivity in the East-Equatorial South Atlantic: Response to changes in trade/monsoon wind forcing and surface water advection, in *The South Atlantic: Present and Past Circulation*, edited by G. Wefer et al., pp. 527-551, Springer-Verlag, New York, 1996.
- Shackleton, N. J., and N. G. Pisias, Atmospheric carbon dioxide, orbital forcing, and climate, in *The Carbon Cycle and Atmospheric CO₂: Natural Variations Archean to Present*, *Geophys. Monogr. Ser.*, vol. 32, edited by E. Sundquist and W. S. Broecker, pp. 303-317, AGU, Washington, D. C., 1985.
- Short, D. A., J. G. Mengel, T. J. Crowley, W. T. Hyde, and G. R. North, Filtering of Milankovitch cycles by Earth's geography, *Quat. Res.*, *35*, 157-173, 1991.
- Waelbroeck, C., J. Jouzel, L. Labeyrie, C. Lorius, M. Labracherie, M. Stiévenard, and N. I. Barkov, A comparison of the Vostok ice deuterium record and series from Southern Ocean core MD 88-770 over the last two glacial-interglacial cycles, *Clim. Dyn.*, *12*, 113-123, 1995.
- Webb, T. I., W. F. Ruddiman, F. A. Street-Perrott, V. Markgraf, J. E. Kutzbach, P. J. Bartlein, H. E. Wright Jr., and W. L. Prell, Climatic changes during the past 18,000 years: Regional syntheses, mechanisms, and causes, in *Global Climates Since the Last Glacial Maximum*, edited by H. E. Wright Jr. et al., pp. 514-535, Univ. of Minnesota Press, Minneapolis, 1993.
- Whitworth, T., III, and W. D. Nowlin Jr., Water masses and currents of the Southern Ocean at Greenwich meridian, *J. Geophys. Res.*, *92*, 6462-6476, 1987.
- Zielinski, U., R. Gersonde, R. Sieger, and D. Fütterer, Quaternary surface water temperature estimations: Calibration of a diatom transfer function for the Southern Ocean, *Paleoceanography*, *13*, 365-383, 1998.

A. Abelman, Alfred Wegener Institute for Polar and Marine Research, Columbusstraße, 27568 Bremerhaven, Germany. (e-mail: aabelmann@awi-bremerhaven.de)

U. Brathauer, GeoForschungsZentrum Potsdam, Telegrafenberg, 14473 Potsdam, Germany. (e-mail: brath@gfz-potsdam.de)

(Received May 13, 1998;
revised November 17, 1998;
accepted November 17, 1998.)